JOURNAL OF MATERIALS SCIENCE 26 (1991) 2573–2578

Characterization of aluminium-matrix composites made by compocasting and its variations

PRASHANT G. KARANDIKAR, TSU-WEI CHOU
Center for Composite Materials, Department of Mechanical Engineering and Materials Science Program, University of Delaware, Newark, Delaware 19716, USA

Compocasting (semisolid–semisolid, SS) and its two variations: SL (semisolid–liquid) and LL (liquid–liquid) process routes are used to make 2024Al reinforced with 3 mm and 12 mm long FP-alumina fibres. Squeeze-casting is used as a complementary casting technique. The effect of processing route on microstructure and the mechanical properties of these composites is studied. The SS route produces composites with uniform fibre distribution, but casting is difficult due to the high viscosity of the slurry. The SL route gives good fibre distribution and the casting is easy. The LL route allows addition of a large amount of fibres but gives castings with a non-uniform fibre distribution, which lowers the failure strains and reduces the strength of the composites drastically. The addition of alumina fibres to 2024Al increases its modulus of elasticity considerably. The observed modulus values show good agreement with the theoretical predictions. The strength values are somewhat lower than the theoretical predictions. This is because the composites failed at strains slightly lower than the fibre failure strain. Absence of fibre pull-out indicates that a good fibre matrix bond has been produced in each case.

1. Introduction

Aluminium matrix composites reinforced with discontinuous FP (Du Pont, Delaware) alumina fibres are made in this work by compocasting. Unfortunately the fibres are wetted very poorly by aluminium. Liquid aluminium always has a thin layer of alumina on its surface. This is shown to be the primary reason for poor wetting between liquid aluminium and different reinforcements [1]. Various methods have been suggested for improving wetting and controlling the reactions between aluminium and the reinforcements. These include: alloying additions [2, 3], reinforcement coating [2–5], melt superheat [1], mechanical methods (compocasting), and pressure casting [6].

Compocasting [7, 8] is a process for making discontinuously reinforced metal-matrix composites. In this process the reinforcement is added to a semisolid matrix alloy and the mixture is agitated vigorously. The agitation repeatedly breaks the alumina skin formed on the surface of liquid aluminium and brings it in intimate contact with the reinforcement. The reinforcement is also trapped by the primary solid phase and prevented from agglomerating. When sufficient mixing is produced the composite slurry is cast. This method is referred to as SS (semisolid–semisolid) [9, 10] in this study. The letters refer to the state of the matrix during the two manufacturing steps: mixing and casting. Three major drawbacks of the SS process are: fibre breakage, porosity, and processing difficulties due to high viscosity.

Two variations of the compocasting process [8, 10] have been suggested to overcome some of the above-mentioned drawbacks. These variations are SL (semisolid–liquid) and LL (liquid–liquid) process routes. Fig. 1 shows the basic compocasting process and its variations. Composites have been made by all three routes to find out how the processing route affects the composite morphology and mechanical properties. The composite slurries are cast under pressure. Most of the porosity is eliminated due to the pressure applied during casting. Pressure also refines the matrix microstructure [11], breaks down the dendritic structure, and improves wetting of the fibres by the matrix [6].

The microstructure of the composites produced by compocasting is affected to a great extent by the

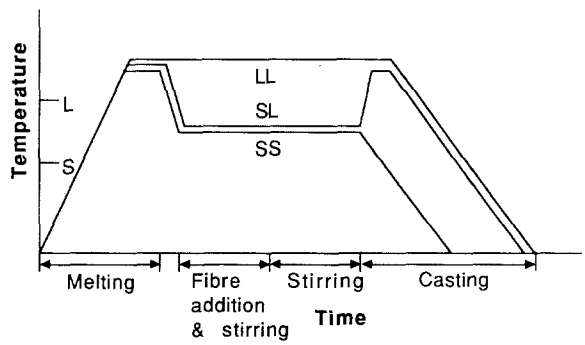

Figure 1 Compocasting (SS: semisolid–semisolid) and its variations SL (semisolid–liquid) and LL (liquid–liquid). L = liquidus, S = solidus.

0022–2461/91 $03.00 + .12

TABLE I Processing conditions used in the three process routes

Process route	Metal heating temperature (°C)	Rate of metal cooling to semisolid state (°C sec^{-1})	Temperature of adding fibres (°C)	Shear rate (r.p.m.)	Casting temperature (°C)
SS	700	1.0	630	400	630
SL	700	1.0	630	400	700
LL	700	–	700	400	700

processing conditions. Important microstructural features that must be controlled are: distribution of the reinforcement, matrix microstructure, and porosity. Processing variables [8, 12, 13] that decide these properties are: apparent viscosity of the slurry, cooling rate from liquid to semisolid state, shear rate during mixing, temperature of the matrix alloy, volume fraction of the primary solid phase, and volume fraction of the reinforcement.

2. Experimental details

FP-alumina fibres were used for reinforcing 2024Al in this work. The fibre mixing device and the squeeze-casting device are the two main components of the set-up. The agitator has to withstand a temperature of 750 °C and resist wear by alumina fibres at that temperature. A steel agitator with hard facing was found to give satisfactory performance. An existing heat press was modified to do pressure diecasting.

Fibre addition, mixing, and casting under pressure are the three major steps in the manufacturing. Table I gives the temperatures at which these three operations are performed in the three process routes mentioned above. In the SS route the fibres are added to a semisolid matrix, mixed, and the slurry is cast while the matrix is still semisolid. The cooling rate from the liquid state to the semisolid state is important as it decides the primary globule size. In the SL route fibres are added to a semisolid matrix and mixed. After this step the slurry is reheated quickly to melt the matrix and then it is cast. In the LL route the fibres are added to a liquid matrix, mixed, and then the slurry is cast. Mould temperature is 450 °C. The slurries are cast under a pressure of 50 MPa. The mixing time is usually about 30 min. A stirring speed of 400 r.p.m. is used. Adequate mixing is achieved at this speed without making the flow turbulent. The time-lag between the pouring of the metal and application of the pressure has to be minimized to avoid solidification before application of the pressure. The SL and LL routes are more forgiving in this respect, as the slurry has a higher superheat compared to the SS route.

A typical casting is 19.1 mm × 76.2 mm × 76.2 mm in dimensions. Twelve tensile test specimens are machined from each casting. These are plate-type samples (3 mm × 15 mm × 70 mm). The density of each test sample is calculated by measuring its weight (±0.5%) and volume (±0.25%). Samples cut from the same casting show different densities due to the varying fibre content. The standard deviation of these density values is calculated for each casting. A higher standard deviation indicates a higher variation in fibre content, and hence higher non-uniformity of fibre distribution. The castings are made by squeeze-casting and the porosity content is small. Hence the density values can be used to calculate the fibre content in each test sample according to the rule of mixtures. These samples are tensile tested at a crosshead speed of 0.15 mm sec^{-1}.

The samples are observed under optical and scanning electron microscopes. Energy-dispersive X-ray analysis (EDAX) is performed on the samples to identify microscopic features. The fracture surfaces of the composites are studied with the scanning electron microscope to identify the nature of failure.

3. Results and discussion

3.1. Morphological characterization

The composite microstructure is affected strongly by the processing conditions which change with the processing route (SS, SL, LL). Table II shows the processing route used for making each casting. All the properties have been given in terms of casting numbers to enable comparison of the three process routes. The standard deviation of density in each casting is also given in Table II. Consider the composites with 3 mm long fibres. As the process route changes from SS to SL to LL, the variation in the density increases. The increase is small when the process changes from SS to SL, but is significant when it changes from SL to LL. This large increase in density variation in going from SL to LL can also be seen in the case of composites with 12 mm fibres.

In the SS process, fibres are added to a semisolid matrix and the mixture is agitated. The primary solid globules deagglomerate the fibres and disperse them uniformly in the liquid around the globules. The alumina skin formed on liquid aluminium is broken and fresh unoxidized aluminium is exposed, which wets the fibres. Once wetted, the fibres stay well dispersed and do not settle or cluster in the presence of primary solid phase. The mixture is cast when the

TABLE II Processing route used for each casting and dependence of density variation (fibre distribution) on processing route

Casting No.	Fibre length (mm)	Processing route	Standard deviation of density
5	12	SL	0.0252
12		SL	0.0396
22		LL	0.0764
29	3	SS	0.0408
25		SL	0.0412
27		LL	0.0654

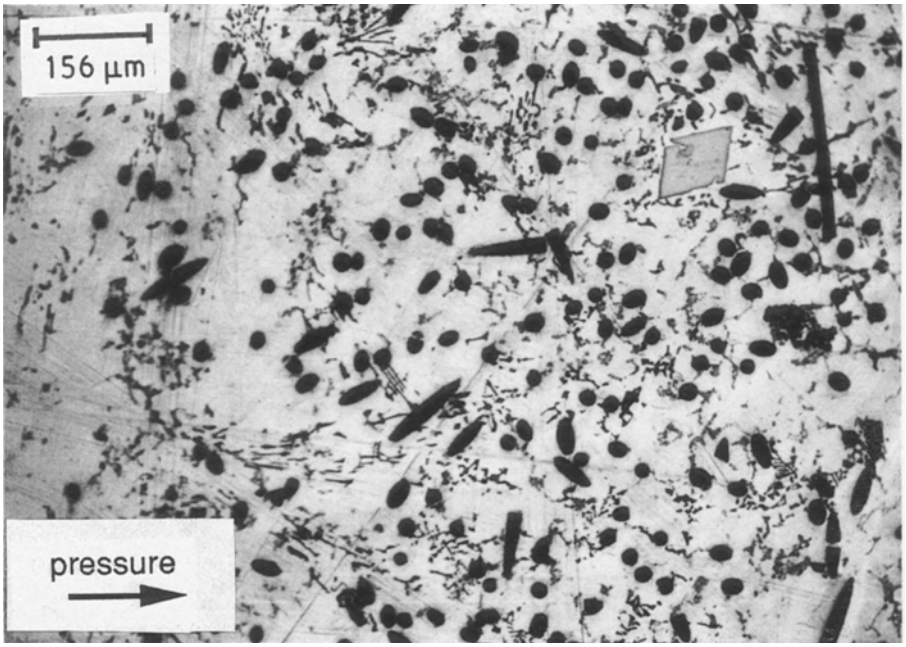

Figure 2 Microstructure of 2024Al reinforced with 3 mm FP-alumina fibres: process route SS, $V_f = 9\%$.

matrix is still in the semisolid state. Thus the fibre distribution in the final composites is uniform as seen in Fig. 2. This results in only small variations in density. Fig. 2 also shows that the castings produced by this method have globular microstructure. In the SS route large amount of air can be entrapped due to the high slurry viscosity, but squeeze-casting eliminates the porosity.

In the SL route, the mixing step is same as in the above case. Thus a mixture with good fibre distribution is produced. This slurry is reheated to melt the matrix before casting. As the slurry temperature increases, the number of primary solid globules decreases and fibres get a chance to agglomerate. If the time-lag between mixing and casting is kept small, it leads to only a small increase in density variation which can be verified in Fig. 3. The matrix microstructure in this case is broken dendritic.

In the LL route, fibres are added to a completely liquid matrix. The primary solid phase is not present to disperse the fibres. Thus the fibre distribution produced in the slurry itself is non-uniform. This non-uniform distribution is carried over to the final castings. Thus the castings produced by this route should show a large variation in density, which indeed is the case as seen in Fig. 4. The composites made by this route are less susceptible to air entrapment during mixing. The fibres are also less susceptible to breakage in this route as the primary solid phase is absent.

In the micrographs shown in Figs 2 to 4, the direction of the applied pressure is also indicated. The fibres seem to be oriented preferentially in the direction perpendicular to the pressure. Thus a two-dimensional random fibre distribution has been produced. In all the cases, copper has been found (through EDAX analysis) to segregate in the interface

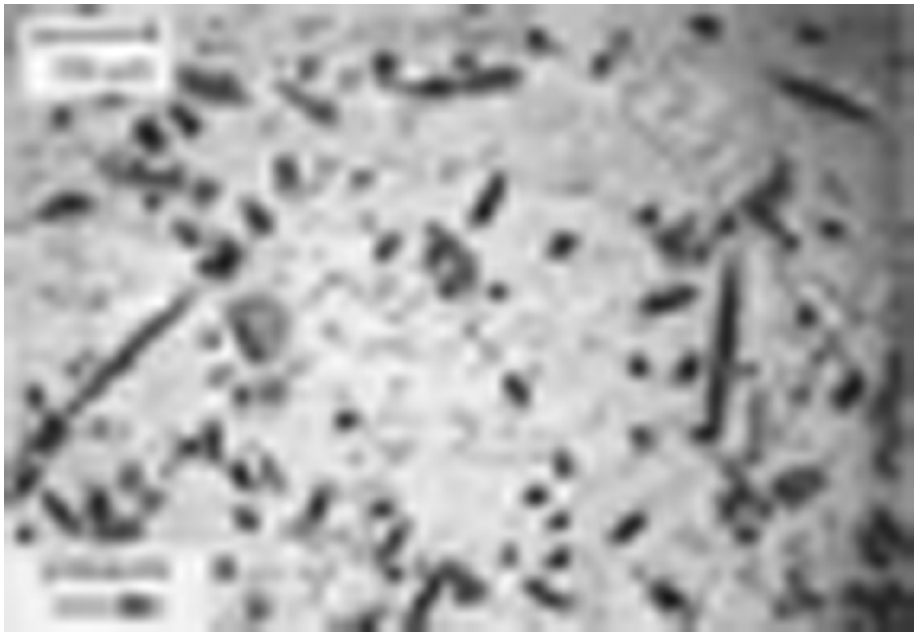

Figure 3 Microstructure of 2024Al reinforced with 12 mm FP-alumina fibres: process route SL, $V_f = 9\%$.

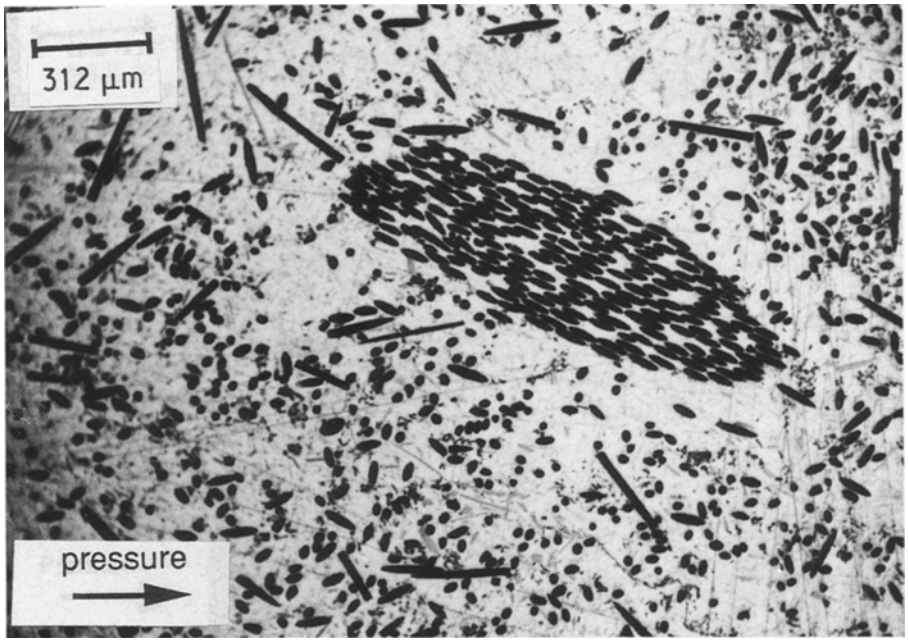

Figure 4 Microstructure of 2024Al reinforced with 12 mm FP-alumina fibres: process route LL, $V_f = 19\%$.

region. Segregation of alloying elements, along with the presence of fibres, makes the heat-treatment kinetics of the composites different from that of the matrix [14].

3.2. Mechanical characterization

Addition of fibres results in a considerable increase in the modulus of elasticity for both types of composites (3 and 12 mm long fibres). Fig. 5 shows the modulus of elasticity against fibre volume percentage for 3 mm long and 12 mm long FP-alumina fibre composites. The modulus of elasticity increases as the fibre volume fraction increases. Up to 75% increase in the modulus has been obtained for a reinforcement content of 30% in both cases. The increase in the modulus is independent of fibre length. Below a critical fibre length the modulus is affected by fibre length, but above the critical value the modulus becomes independent of fibre length. This indicates that both types of fibre used here must be longer than the critical length. This can be verified by calculating the critical fibre length for this system. Fibre critical length (l_c) is given by the following expression [15]:

$$l_c = \frac{\sigma_{uf} d}{2\tau} \quad (1)$$

where σ_{uf} is the ultimate tensile strength of the fibre, d is the diameter of the fibre and τ is the interfacial shear strength which is assumed to be equal to half the tensile yield strength (78 MPa) of the matrix.

Substituting the appropriate values into Equation 1 gives a critical length of 360 μm. The fibres used are 3000 and 12000 μm long. These are considerably longer than the critical length and will be longer than the critical length even after processing, which can reduce the fibre length considerably (as much as 25% reduction). Thus the observed increase in modulus due to both types of fibres is consistent with theory. The modulus of these composites can be calculated theoretically by considering a two-dimensional (2-D) random distribution of long fibres in the matrix. The modulus is given by [15]

$$E = 2\pi \int_0^{\pi/2} E(\theta) d\theta \quad (2)$$

$E(\theta)$ is the modulus of a unidirectional composite with

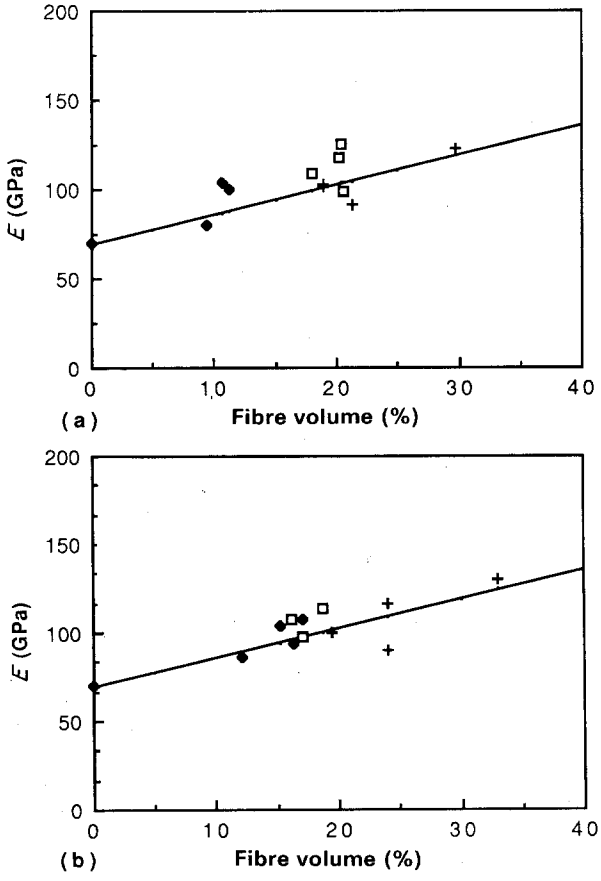

Figure 5 Modulus of elasticity against V_f for 2024Al. (a) 3 mm long FP-alumina fibres: (◆) cast 29, (□) cast 25, (+) cast 27, (—) theoretical. (b) 12 mm fibres: (◆) cast 5, (□) cast 12, (+) cast 22, (—) theoretical.

the fibres at an angle θ to the loading direction and the same volume fraction V_f as the random fibre composite. The actual calculation from this formula is tedious. A reasonably accurate modulus value for a composite with a particular volume fraction of fibres can be calculated by using the following expression [15]:

$$E = \frac{3}{8}E_{\parallel} + \frac{5}{8}E_{\perp} \quad (3)$$

Here $E_{\parallel}$ is the modulus of elasticity of unidirectionally reinforced composites with the same V_f as the random fibre composite and in which the fibres are parallel to the loading direction. $E_{\perp}$ is the modulus of elasticity of unidirectionally reinforced composites with the same V_f as the random fibre composite and in which the fibres are perpendicular to the loading direction. The calculated values are shown by a line in Fig. 5 and agree well with the experimentally measured values.

Fig. 6 shows the variation of the ultimate tensile strength (UTS) with volume percentage of fibres for 3 and 12 mm long FP-alumina fibre composites (as-cast condition). Friend [16] has proposed a theory to predict the strength of discontinuously reinforced metal matrix composites. A theoretical expression for the UTS is obtained by modifying the expression for continuous fibre composites. This is done by introducing factors which account for the finite length and random orientation distribution of the fibres:

$$\sigma_c = b\sigma_{uf}V_f\left(1 - \frac{l_c}{2l}\right) + \sigma_m^*(1 - V_f) \quad (4)$$

where $b = 3/8$ for 2-D (or transversely) isotropic fibre distribution, $b = 1/5$ for 3-D isotropic fibre distribution, σ_c is the composite strength, σ_{uf} is the ultimate tensile strength of the fibres (1379 MPa), σ_m^* is the matrix strength at fibre failure strain (160 MPa), l and l_c are fibre length and fibre critical length, respectively, σ_{um} is the UTS (200 MPa) of the matrix and V_f is the volume fraction of the fibres.

The fibre distribution is 2-D isotropic for composites made in this work. Hence the former value of b is chosen. The residual matrix strength is given by the equation

$$\sigma = \sigma_{um}(1 - V_f) \quad (5)$$

Thus Equations 4 and 5 give the composite strength. These two equations have been plotted along with the experimental values in Fig. 6.

The experimental values are lower than the theoretically predicted values. In the above predictions a composite is assumed to fail when the strain reaches fibre failure strain. The composite failure strains are shown in Fig. 7. It can be seen that composite failure strains are lower than fibre failure strain (0.37%). This phenomenon is responsible for the observed lower

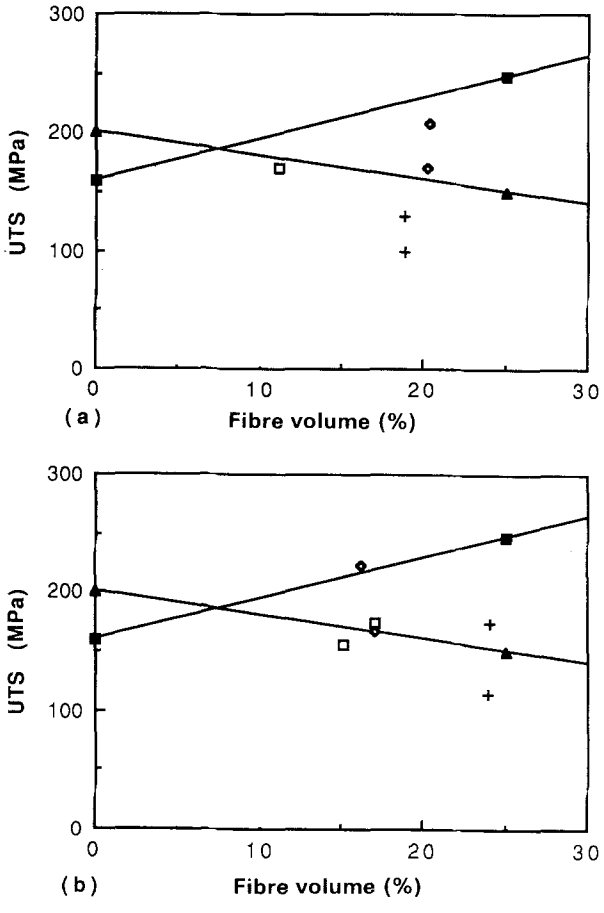

Figure 6 UTS against V_f for 2024Al. (a) 3 mm long FP-alumina fibres: (□) cast 29, (◇) cast 25, (+) cast 27, (■) Equation 4, (▲) Equation 5. (b) 12 mm fibres: (□) cast 5, (◇) cast 12, (+) cast 22, (■) Equation 4, (▲) Equation 5.

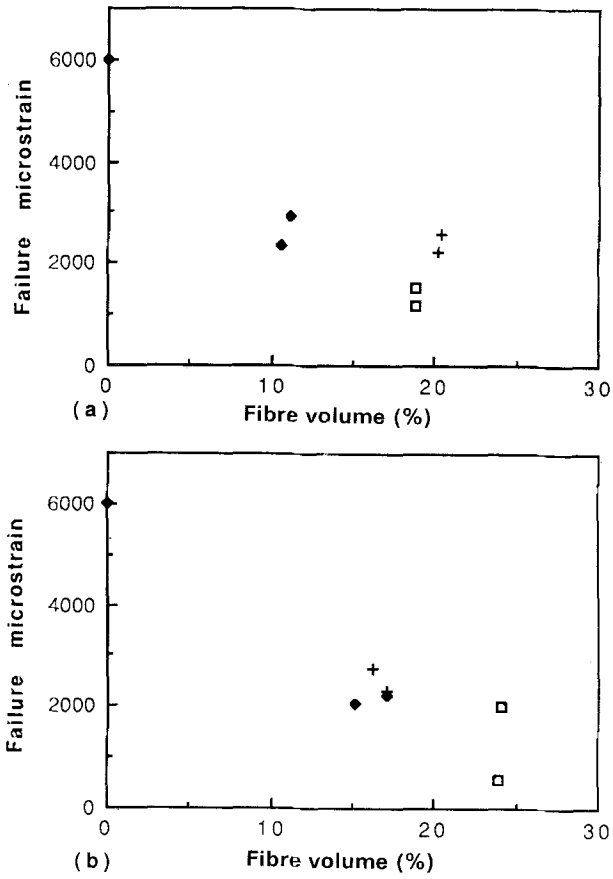

Figure 7 Failure microstrain against V_f for 2024Al. (a) 3 mm long FP-alumina fibres: (□) cast 27, (◆) cast 29, (+) cast 25. (b) 12 mm fibres: (□) cast 22, (◆) cast 5, (+) cast 12.

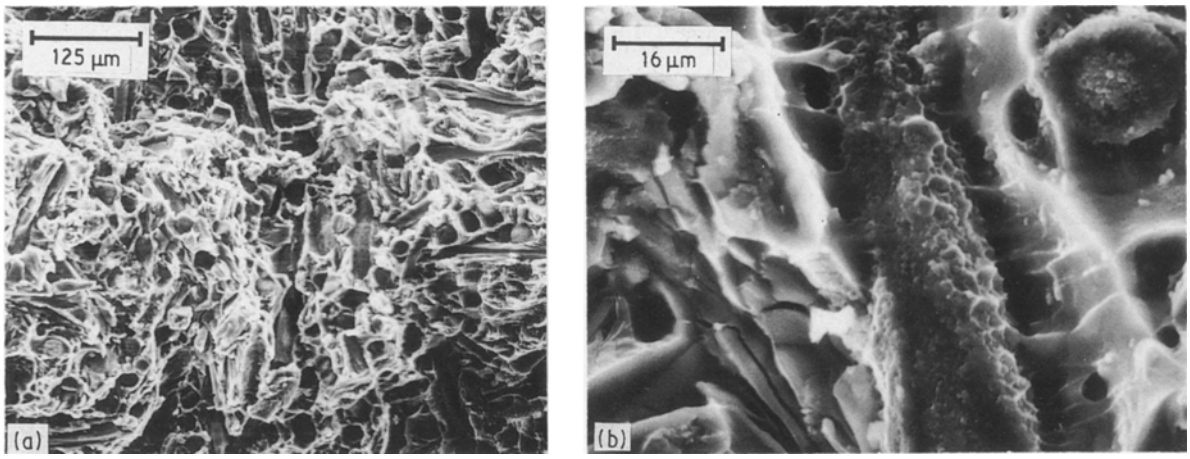

Figure 8 Tensile fracture surface of 2024Al–FP-alumina composites: process route LL, 3 mm long fibres, $V_f = 19\%$; (a, b) two magnifications.

strengths. This conclusion is further supported by the fact that composite samples with lower failure strains show lower strengths (compare Figs 6 and 7). Thus composite failure strain is a very important parameter which decides the strength of the composite.

Casting Nos 27 and 22 produced by the LL route show low failure strains. It has been shown before that the LL process route gives castings with non-uniform fibre distribution and fibre clustering. These are the major reasons for the lower failure strains shown by these castings. Thus if castings have to be made by this route, fibre clustering must be prevented.

A typical tensile fracture surface is shown in Fig. 8. No fibre pull-out is seen. Composites produced by all three routes show similar behaviour. This indicates that a good fibre–matrix bond has been produced in composites made by all three routes. Since the composites have been squeeze-cast, the pressure applied during solidification may also be partly responsible for the good bond produced. This indicates that in this manufacturing procedure the matrix does not have to be in a semisolid phase to produce a good fibre–matrix bond.

4. Conclusions

Compocasting (SS) and its two variations can be used successfully to make discontinuously reinforced metal-matrix composites. When combined with squeeze-casting, all three process routes give composites with good fibre–matrix bond and low porosity.

Each of these process routes has its own advantages and disadvantages. The SS route gives composites with uniform fibre distribution but poses problems during casting. A larger amount of gas entrapment is observed in this case. It is difficult to add a large amount of fibres to a semisolid matrix. The SL route combines the uniform fibre distribution with the ease of casting. The LL route allows addition of a large amount of fibres but cannot disperse the fibres uniformly.

FP-alumina fibres increase the modulus of elasticity of 2024-Al substantially, but the as-cast strength increase is not so significant. This is mainly due to the low failure strain of the composites. The composite failure strain is found to be slightly lower than the fibre failure strain. The composite failure strain varies from sample to sample, and samples with low failure strains show lower strengths. Fibre clustering is the major reason for the reduction of failure strain. Thus the fibre distribution must be closely controlled to get composites with reproducible properties.

Acknowledgements

The authors wish to thank Dr Frank Girot for his help during setting up of the experiments. The authors also wish to thank the Office of Naval Research (Dr L. H. Peebles Jr, Program Director) and the Center for Composite Materials, University of Delaware for partial support of the work.

References

1. N. EUSTATHOPOULOS, J. C. JOUD, P. DESRE and J. M. HICTER, *J. Mater. Sci.* **9** (1974) 1233.
2. Y. KIMURA, *J. Mater. Sci.* **19** (1984) 3107.
3. A. R. CHAMPION, W. H. KRUEGER, H. S. HARTMAN and A. K. DHINGRA, in Proceedings of the 2nd ICCM, Toronto, April, 1978, edited by B. R. Noton (Metallurgical Society of AIME, Warrendale,1978) p. 883.
4. A. G. KULKARNI, B. C. PAI and N. BALASUBRAMANIAN, *J. Mater. Sci.* **14** (1979) 592.
5. H. K. KATZMAN, *ibid.* **22** (1987) 144.
6. B. K. PRASAD, T. K. DAN and P. K. ROHATGI, *J. Mater. Sci. Lett.* **6** (1987) 1076.
7. R. MEHRABIAN, R. G. RIEK and M. C. FLEMINGS, *Met. Trans.* **5** (1974) 1899.
8. F. GIROT, PhD thesis, University of Bordeaux, France (1987).
9. B. F. QUIGLEY, G. J. ABBASCHIAN, R. WUNDERLIN and R. MEHRABIAN, *Met. Trans. A* **13** (1982) 93.
10. A. MUNITZ, M. METZGER and R. MEHRABIAN, *ibid.* **10** (1979) 1491.
11. T. W. CHOU, A. KELLY and A. OKURA, *Composites* **16** (1985) 187.
12. P. A. JOLY and R. MEHRABIAN, *J. Mater. Sci.* **11** (1976) 1393.
13. F. GIROT, P. G. KARANDIKAR, T. W. CHOU and A. MAJIDI, in "Materials Pathway to the Future", edited by G. Corrillo *et al.* (Sampe Corina, CA, 1988) p. 1260.
14. C. M. FRIEND and S. D. LUXTON, *J. Mater. Sci.* **23** (1988) 3173.
15. D. HULL, "Introduction to Composite Materials" (Cambridge University Press, 1981) p. 91.
16. C. M. FRIEND, *J. Mater. Sci.* **22** (1987) 3005.

Received 1 August 1989
and accepted 19 February 1990